

Measuring small longitudinal phase shifts via weak measurement amplification

Kai Xu(徐凯), Xiao-Min Hu(胡晓敏), Meng-Jun Hu(胡孟军), Ning-Ning Wang(王宁宁), Chao Zhang(张超), Yun-Feng Huang(黄运锋), Bi-Heng Liu(柳必恒), Chuan-Feng Li(李传锋), Guang-Can Guo(郭光灿), and Yong-Sheng Zhang(张永生)

Citation: Chin. Phys. B, 2024, 33 (**3**): 030602. DOI: 10.1088/1674-1056/ad1c5a
Journal homepage: http://cpb.iphy.ac.cn; http://iopscience.iop.org/cpb

What follows is a list of articles you may be interested in

Robust free-space optical frequency transfer in time-varying link distances conditions

Zhou Tong(童周), Lei Liu(刘雷), Jia-Liang Wang(王家亮), Qian Cao(操前), Zhi-Cheng Jin(金志成), Kang Ying(应康), Shen-Sheng Han(韩申生), Zheng-Fu Han(韩正甫), and You-Zhen Gui(桂有珍)

Chin. Phys. B, 2024, 33 (**2**): 020601. DOI: 10.1088/1674-1056/ad0718

Multilevel atomic Ramsey interferometry for precise parameter estimations

X N Feng(冯夏宁) and L F Wei(韦联福)

Chin. Phys. B, 2021, 30 (**12**): 120601. DOI: 10.1088/1674-1056/ac0527

Signal-recycled weak measurement for ultrasensitive velocity estimation

Sen-Zhi Fang(方森智), Yang Dai(戴阳), Qian-Wen Jiang(姜倩文), Hua-Tang Tan(谭华堂), Gao-Xiang Li(李高翔), and Qing-Lin Wu(吴青林)

Chin. Phys. B, 2021, 30 (**6**): 060601. DOI: 10.1088/1674-1056/abda2d

Enhancing the precision of phase estimation by weak measurement and quantum measurement reversal

He Zhi (贺志), Yao Chun-Mei (姚春梅)

Chin. Phys. B, 2014, 23 (**11**): 110601. DOI: 10.1088/1674-1056/23/11/110601

Quantum metrology

Xiang Guo-Yong (项国勇), Guo Guang-Can (郭光灿)

Chin. Phys. B, 2013, 22 (**11**): 110601. DOI: 10.1088/1674-1056/22/11/110601

RAPID COMMUNICATION

Measuring small longitudinal phase shifts via weak measurement amplification

Kai Xu(徐凯)[1,2], Xiao-Min Hu(胡晓敏)[1,2,3], Meng-Jun Hu(胡孟军)[4,†], Ning-Ning Wang(王宁宁)[1,2,3], Chao Zhang(张超)[1,2,3], Yun-Feng Huang(黄运锋)[1,2,3], Bi-Heng Liu(柳必恒)[1,2,3,‡], Chuan-Feng Li(李传锋)[1,2,3,§], Guang-Can Guo(郭光灿)[1,2,3], and Yong-Sheng Zhang(张永生)[1,2,3,¶]

[1] *CAS Key Laboratory of Quantum Information, University of Science and Technology of China, Hefei* 230026, *China*
[2] *CAS Center For Excellence in Quantum Information and Quantum Physics, University of Science and Technology of China, Hefei* 230026, *China*
[3] *Hefei National Laboratory, University of Science and Technology of China, Hefei* 230088, *China*
[4] *Beijing Academy of Quantum Information Sciences, Beijing* 100193, *China*

(Received 22 November 2023; revised manuscript received 7 January 2024; accepted manuscript online 9 January 2024)

Weak measurement amplification, which is considered as a very promising scheme in precision measurement, has been applied to various small physical quantities estimations. Since many physical quantities can be converted into phase signals, it is interesting and important to consider measuring small longitudinal phase shifts by using weak measurement. Here, we propose and experimentally demonstrate a novel weak measurement amplification-based small longitudinal phase estimation, which is suitable for polarization interferometry. We realize one order of magnitude amplification measurement of a small phase signal directly introduced by a liquid crystal variable retarder and show that it is robust to the imperfection of interference. Besides, we analyze the effect of magnification error which is never considered in the previous works, and find the constraint on the magnification. Our results may find important applications in high-precision measurements, e.g., gravitational wave detection.

Keywords: weak measurement, phase estimation, quantum optics

PACS: 06.20.–f, 42.50.–p **DOI:** 10.1088/1674-1056/ad1c5a

1. Introduction

Weak measurement, which was first proposed by Aharonov, Albert, and Vaidman,[1] has attracted a lot of attention in the last decades.[2] In the theoretical framework of weak measurements, the system with a pre-selected state interacts weakly with the pointer first and then followed by a post-selection on its state. When the interaction is weak enough so that only the first-order approximation needs to be considered, the so-called weak value of observable $\hat{A}$, defined as $\langle\hat{A}\rangle_{\rm w} = \langle\psi_{\rm i}|\hat{A}|\psi_{\rm f}\rangle/\langle\psi_{\rm i}|\psi_{\rm f}\rangle$ with $|\psi_{\rm i}\rangle$ and $|\psi_{\rm f}\rangle$ being the pre-selected state and post-selected state of the system, respectively, emerges naturally in the framework of weak measurements.[1] The weak value is generally complex, with its real part and imaginary part being obtained separately by performing measurement of non-commuting observables on the pointer,[3] and can be arbitrarily large when $|\psi_{\rm i}\rangle$ and $|\psi_{\rm f}\rangle$ are almost orthogonal. Although the weak value has been intensively investigated since its birth,[4–7] the debate on its physical meaning continues.[8–13] Regardless of these arguments, the method of weak measurement has been shown powerful in solving quantum paradox,[14–16] reconstructing quantum state,[17–20] amplifying small effects[21–25] and investigating foundations of the quantum world.[26–31]

Among the above applications, weak value amplification (WVA) is particularly intriguing and has been rapidly developed in high-precision measurements. In order to realize WVA, the tiny quantity to be measured needs to be converted into the coupling coefficient of a von Neumann-type interaction Hamiltonian, which is small enough so that the condition of weak measurements is satisfied. The magnification of WVA is directly determined by the weak value of the system observable appearing in the interaction Hamiltonian. When the pre-selected state $|\psi_{\rm i}\rangle$ and the post-selected state $|\psi_{\rm f}\rangle$ of the system are properly chosen, the weak value can be arbitrarily large. However, the magnification is limited when all orders of evolution are taken into consideration.[32–35] While the potential application of the weak value in signal amplification was pointed out as early as 1990,[36] it has drawn no particular attention until the first report on the observation of the spin Hall effect of light via WVA.[21] Since then, many kinds of signal measurements via WVA have been reported, such as geometric phase,[37] angular rotation,[38,39] spin Hall effect,[21,40–42] single-photon nonlinearity,[43–46] frequency,[47,48] etc.

Despite those progresses in experiments, WMA obtains

†Corresponding author. E-mail: humj@baqis.ac.cn
‡Corresponding author. E-mail: bhliu@ustc.edu.cn
§Corresponding author. E-mail: cfli@ustc.edu.cn
¶Corresponding author. E-mail: yshzhang@ustc.edu.cn

© 2024 Chinese Physical Society and IOP Publishing Ltd

the large weak value at the price of low detection probability by post-selection, which may cause greater overall error.[49] Therefore, the controversy on whether or not WVA outperforms conventional measurements (CM) arises.[50–55] Several theoretical articles reveal that the post-selection process loses some information, which can reduce the quantum Fisher information (QFI) and result in poorer overall precision than the CM.[56–58] However, advantages arise when practical experiments are taken into consideration. There are some works showing that WMA has the robustness to technical noise.[59–61] Meanwhile, some technical advantages of WVA have been experimentally demonstrated.[62–65] The reason for this contradiction is that the theoretical analysis ignores some practical constraints, which may dominate the error of experiment results. In the experiment, the signal is amplified while the technical noise remains constant. Therefore, the signal-to-noise ratio is boosted by a factor determined by the weak value.[66] There were many attempts of WVA-based proposals for further improvement of the precision, including optimization of pointer states such as squeezing[55] and entanglement,[67,68] the utilization of the recycling technique,[69–72] iterative interactions,[73] and the almost-balanced weak-value amplification technique.[74–76]

Since many physical quantities can be converted into phase measurements, using WVA to realize small phase measurement, especially longitudinal phase, has been developed rapidly.[77–81] However, previous schemes are still not suitable for practical applications because of their severe requirements on the preparation of the initial state of the probe with the continuous degree of freedom and detections on time or frequency domain. The direct amplification of the phase shift in optical interferometry with weak measurement has been experimentally studied by Li *et al.*[82] The final phase shifts are calculated by scanning the oscillation patterns without and with weak measurement. However, the amplified phase cannot be obtained quickly and their scheme does not apply to the longitudinal phase. Here we propose a different scheme of small longitudinal phase amplification measurement within the framework of weak measurements. Compared with the Sagnac interferometer scheme in Ref. [82], it is universal and can be used in other interferometers like the Michelson interferometer suggested in Refs. [83,84].

In this article, we experimentally demonstrate this new scheme by measuring a small longitudinal phase caused by the liquid crystal variable retarder and realizing one order of magnitude amplification. Besides, the previous theoretical and experimental works do not consider the effect of magnification errors when doing error analysis. In this paper, we add this part and find that the magnification error gradually increases and becomes dominant as the weak value increases. We obtain the trade-off between the weak value magnification and measurement accuracy.

2. Weak measurements based phase amplification

The key idea of weak measurements based small phase amplification (WMPA) is to transform the small longitudinal phase to be measured into a larger rotation along the latitude of the Bloch sphere of the meter qubit, e.g., larger rotation of a photon's polarization.[83] To explicitly see how it works, consider a two-level system initially prepared in the state of superposition $|\psi_{\rm i}\rangle_{\rm S}=\alpha|0\rangle+\beta|1\rangle$ with $|\alpha|^2+|\beta|^2=1$. Contrary to most discussions of WVA in which continuous pointer is used,[1,2,21,22] we adopt discrete pointer $|\phi\rangle_{\rm P}=\mu|\uparrow\rangle+\nu|\downarrow\rangle$ with $|\mu|^2+|\nu|^2=1$. The pointer can be another two-level system or a different degree of freedom of the same system. We consider a unitary control-rotation evolution of the system-pointer interaction

$$\hat{U}=|0\rangle\langle 0|\otimes\hat{I}+|1\rangle\langle 1|\otimes(|\uparrow\rangle\langle\uparrow|+{\rm e}^{{\rm i}\theta}|\downarrow\rangle\langle\downarrow|), \tag{1}$$

where θ is the small phase signal to be measured. After the evolution of the composite system, a post-selection measurement is performed on the system that collapses it into the state $|\psi_{\rm f}\rangle_{\rm S}=\gamma|0\rangle+\eta|1\rangle$ with $|\gamma|^2+|\eta|^2=1$. The state of the pointer, after the post-selection of the system, becomes (unnormalized)

$$\begin{aligned}|\tilde{\varphi}\rangle_{\rm P} &= {}_{\rm S}\langle\psi_{\rm f}|\hat{U}|\psi_{\rm i}\rangle_{\rm S}\otimes|\phi\rangle_{\rm P}\\ &= \mu(\alpha\gamma+\beta\eta)|\uparrow\rangle+\nu(\alpha\gamma+\beta\eta\,{\rm e}^{{\rm i}\theta})|\downarrow\rangle\end{aligned} \tag{2}$$

with the successful probability $P_{\rm s}={\rm Tr}[|\tilde{\varphi}\rangle_{\rm P}\langle\tilde{\varphi}|]$, where α,β,γ,η are all taken to be real numbers without loss of generality. Since $\theta\ll 1$, $\alpha\gamma+\beta\eta\,{\rm e}^{{\rm i}\theta}\simeq(\alpha\gamma+\beta\eta)\,{\rm e}^{{\rm i}\kappa}$ in the first order approximation with

$$\tan(\kappa)=\frac{\sin\theta}{\cos\theta+(\alpha\gamma)/(\beta\eta)}. \tag{3}$$

Since our pointer state is discrete and we do not use the weak interaction approximation $\exp(-{\rm i}gA\otimes P)\approx 1-{\rm i}gA\otimes P$ (the operators A and P act on the system and the pointer, respectively), no definite weak value is needed in our case and the magnification is nonlinear. In the traditional standard WVA, the pointer is a wave packet, such as a Gaussian wave packet, which is slightly deformed after coupling. Only through the first-order approximation of the coupling, the shift of the wave packet can be accurately defined. Our scheme uses the polarization as a pointer, and the shift of the pointer angle can be calculated using exact values in theory. Phase signal amplification is realized when the post-selected state is properly chosen such that ${}_{\rm S}\langle\psi_{\rm f}|\psi_{\rm i}\rangle_{\rm S}=\alpha\gamma+\beta\eta\to 0$. The normalized pointer state is

$$|\varphi\rangle_{\rm P}=\mu|\uparrow\rangle+\nu\,{\rm e}^{{\rm i}\kappa}|\downarrow\rangle \tag{4}$$

in the first-order approximation. Figure 1 shows the schematic diagram of our scheme. Analogous to the micrometer, which transforms small displacement into a larger rotation of the circle, our protocol transforms the small phase into a larger rotation of the pointer along the latitude of the Bloch sphere. The amplified phase information κ can be easily extracted by performing proper basis measurement on the pointer. It is intriguing to note that the WMPA seems to work even when

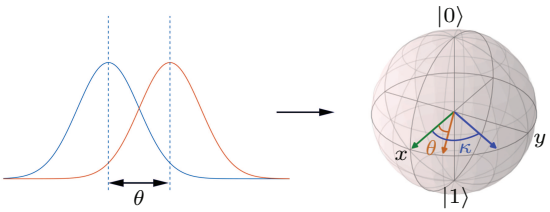


Fig. 1. The schematic diagram of our scheme. The longitudinal phase shift θ (the left) is converted to polarization rotation and is amplified to the phase κ (the right).

${}_{\rm S}\langle\psi_{\rm f}|\psi_{\rm i}\rangle_{\rm S} = 0$, but the approximation of Eq. (3) should be replaced by an accurate one.

3. Experimental realization

In the experimental demonstration shown in Fig. 2, we take the path state of photons as the system and its polarization degree of freedom as the pointer and perform a measurement of the small longitudinal phase introduced by the liquid crystal variable retarder (LCVR). We choose α, β, μ, $\nu = 1/\sqrt{2}$ in our experiment such that the polarization of the post-selected photons is $(|H\rangle + e^{i\kappa}|V\rangle)/\sqrt{2}$ with $|H\rangle$ and $|V\rangle$ representing horizontal and vertical polarizations, respectively. The amplified phase κ is extracted by performing measurement with the basis $\{|+\rangle, |-\rangle\}$ on the post-selected photons, which gives the expected value of the observable $\hat{\sigma}_x \equiv |+\rangle\langle+| - |-\rangle\langle-|$ as $\langle\hat{\sigma}_x\rangle = \cos(\kappa)$, where $|\pm\rangle = (|H\rangle \pm |V\rangle)/\sqrt{2}$.

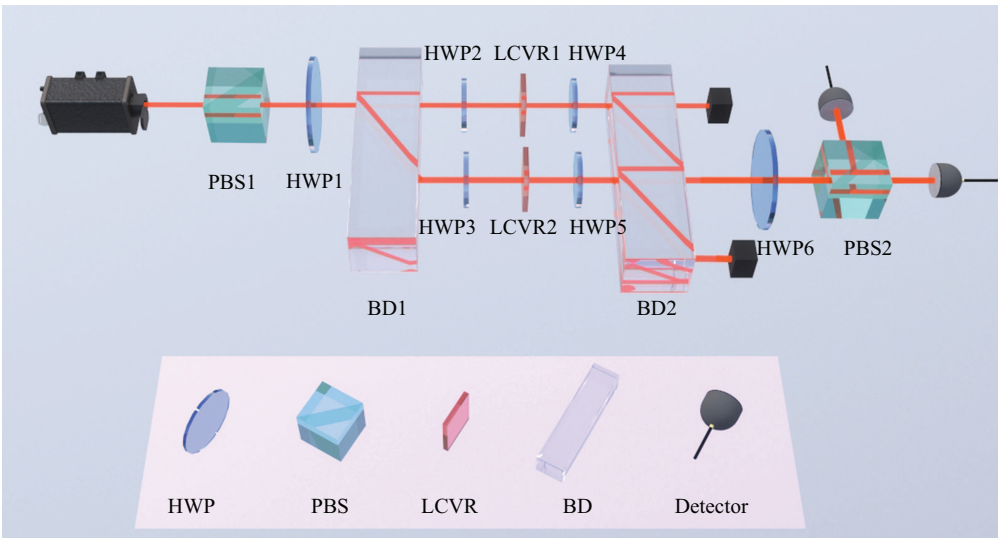


Fig. 2. Experiment setup. An attenuated fiber-coupled laser beam is initially prepared in $|+\rangle$ polarization state by a polarizing beam splitter (PBS) and a half-wave plate (HWP1) rotated at 22.5°. The initial state of the system and the pointer is prepared by a beam displacer (BD) and the HWP2 rotated at 22.5°, the HWP3 rotated at 67.5°, in which the system is the path degree of freedom and the pointer is the polarization degree of freedom. The small phase between horizontal and vertical polarization is produced by the liquid crystal variable retarder (LCVR1) and LCVR2 without voltage added is used for phase compensation. The post-selection of the system is completed by HWP4 rotated at $22.5° - \delta$, HWP5 rotated at $67.5° - \delta$ and a BD with δ being an adjustable small angle to realize different magnification. The amplified phase signal, which is encoded in the polarization state of the post-selected photons, is extracted by a polarization analyzer consisting of the HWP6 rotated at 22.5° and a PBS.

The whole experimental setup consists of four parts, i.e., the initial state preparation, small phase signal θ collection, phase signal amplification via the post-selection, and extraction of the amplified phase signal κ. The small phase θ is derived by substituting the measured κ into the approximation formula of Eq. (3), where $\alpha\gamma/(\beta\eta)$ is the predetermined experimental parameter.

As shown in Fig. 2, the 775 nm laser beam is emitted from the laser. The laser beam has been attenuated before passing through the optical path (it is not drawn in Fig. 2), which results in the final counting rate of approximate 8×10^5 s^{-1}. The light beam passes through a polarizing beam splitter (PBS) and a half-wave plate (HWP1) rotated at 22.5° such that the polarization of photons is prepared in the state $|+\rangle$. Preparation of the initial state of photons is completed by passing through a calcite beam displacer (BD) and two HWPs (HWP2 and HWP3) placed in the two paths separately. The BD is approximately 39.70 mm long and photons with horizontal polarization $|H\rangle$ can transmit through it without change of their path while photons with vertical polarization $|V\rangle$ suffer a 4.21 mm shift away from their original path. The HWP2 and HWP3 are rotated at 22.5° and −22.5°, respectively, which gives the initial state of photons as $(|0\rangle + |1\rangle)/\sqrt{2} \otimes |+\rangle$, where $|0\rangle$ represents the state of down path and $|1\rangle$ represents the state of up path. In fact, the initial state of the system, i.e., path degree of freedom, and the pointer, i.e., polarization degree of

freedom, can be prepared into an arbitrary state via rotating HWP1, HWP2, and HWP3.

The small longitudinal phase signal θ to be measured is produced by LCVR1 (Thorlabs LCC1411-B) placed in the up path. The LCVR causes a phase shift between the horizontal and vertical polarization states of photons when the voltage is introduced by a liquid crystal controller (Thorlabs LCC25), the calibration of LCVR is shown in Appendix B. Another LCVR placed in the down path without introducing voltage is used for phase compensation. The LCVRs fulfill the unitary operation of a controlled rotation and the state of photons, after passing through the LCVRs, becomes

$$|\Psi\rangle_{\rm SP} = \frac{1}{\sqrt{2}}[|0\rangle \otimes |+\rangle + |1\rangle \otimes (|H\rangle + {\rm e}^{{\rm i}\theta}|V\rangle)/\sqrt{2}]. \quad (5)$$

The amplification of the small phase signal θ is completed via HWP4, HWP5, and BD2, where the post-selected photons come out from the middle path of the BD toward HWP6. To see explicitly how post-selection works, we can recast Eq. (5) as

$$\begin{aligned}|\Psi\rangle_{\rm SP} = & \frac{1}{\sqrt{2}}[|H\rangle \otimes (|0\rangle + |1\rangle)/\sqrt{2} \\ & + |V\rangle \otimes (|0\rangle + {\rm e}^{{\rm i}\theta}|1\rangle)/\sqrt{2}],\end{aligned} \quad (6)$$

which implies the exchange of the path degree of freedom and the polarization degree of freedom of photons. Since the polarization degree of freedom of photons represents the system now, post-selection of the system can be readily realized by an HWP combined with a PBS. Suppose that the HWP is rotated at $22.5^\circ - \delta$ with δ being a small angle, then the post-selected state of photons coming out from the reflection port of the PBS is $|\psi_{\rm f}\rangle = \sin(45^\circ - 2\delta)|H\rangle - \cos(45^\circ - 2\delta)|V\rangle$. After the post-selection, we exchange back the system and the pointer to the original degrees of freedom by using an HWP rotated at 45° in one of the outgoing paths and a BD to recombine the light beam. The above process of post-selection can be equivalently realized via HWP4 rotated at $22.5^\circ - \delta$, HWP5 rotated at $67.5^\circ - \delta$ and BD2 as shown in Fig. 2.

The post-selected photons, which come from the middle part of the second BD, are in the polarization state of $|\varphi\rangle_{\rm P} = (|H\rangle + {\rm e}^{{\rm i}\kappa}|V\rangle)/\sqrt{2}$, where κ is the amplified phase signal determined by Eq. (3) with $\alpha = \beta = 1/\sqrt{2}$ and $\gamma = \sin(45^\circ - 2\delta), \eta = -\cos(45^\circ - 2\delta)$. The amplified phase κ can be extracted by performing a measurement with the basis $\{|+\rangle, |-\rangle\}$ and calculating the expected value of Pauli observable $\hat{\sigma}_x$, which is realized by HWP6 rotated at 22.5°, a PBS and two avalanche photodiode single-photon detectors (SPD). Once κ is obtained, the small phase θ can be easily derived from Eq. (3).

4. Results

Figure 3 shows the relationship between the amplified phase κ and the small phase θ, in which lines are theoretical predictions and dots are measured data. When the phase signal to be measured is small enough, according to Eq. (3), the factor of amplification is mainly determined by the parameter $(\alpha\gamma)/(\beta\eta)$. Two different values of $(\alpha\gamma)/(\beta\eta)$ are considered in our experiment corresponding to the magnification factors about 4 and 10 with success probabilities $p = 0.0204$ ($\delta = 0.0716$) and $p = 0.0026$ ($\delta = 0.0255$) respectively in the linear amplification region. For each case, four small phases are chosen in the range between 0.03 rad and 0.08 rad, which are produced by LCVR1 and are measured in advance.

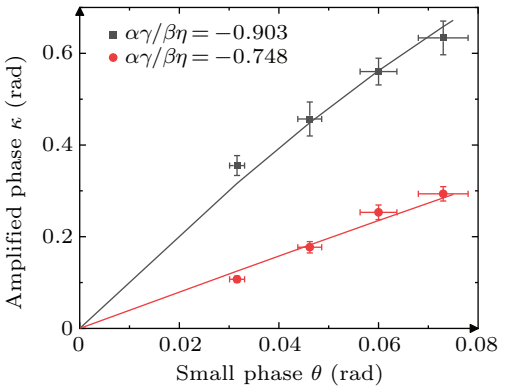


Fig. 3. Experimental results of phase amplification. The relationship between the amplified phase κ and the small phase θ which is to be measured. The real lines are theoretical predictions based on Eq. (3) with different colors representing different values of $(\alpha\gamma)/(\beta\eta)$. The dots are measured data. The transverse errors come from the calibration errors and the longitudinal errors are derived from the raw data.

As an important experimental parameter, $(\alpha\gamma)/(\beta\eta)$ needs to be determined before the amplification measurement. This is done by measuring the successful probability of post-selection, i.e., $p = |\langle\psi_{\rm f}|\psi_{\rm i}\rangle|^2 = (\alpha\gamma + \beta\eta)^2$ without introducing any small phase. In the case of our experiment, $(\alpha\gamma)/(\beta\eta) = -\tan(45^\circ - 2\delta)$ and $\sin(2\delta) = \sqrt{p}$, which gives

$$\frac{\alpha\gamma}{\beta\eta} = \frac{\sqrt{p} - \sqrt{1-p}}{\sqrt{p} + \sqrt{1-p}}. \quad (7)$$

Once the parameter $(\alpha\gamma)/(\beta\eta)$ is settled, the voltage can be added to LCVR to produce a small phase and the amplification measurement can be realized. The small phase θ is immediately estimated by conventional measurement methods after the amplification measurement, which is done by blocking the down path between BDs, replacing HWP4 with an HWP rotated at 67.5° and rotating HWP6 to 45°. Two different values of $(\alpha\gamma)/(\beta\eta)$ are obtained by adjusting the small angle δ and four small phases are measured within 30 s counting for each value. Considering the relevant statistical errors, random errors, and imperfections of optical elements, our results fit well with the theoretical predictions.

As the key part of the experimental setup, the performance of the BD-type Mach–Zehnder interferometer directly determines the precision of phase estimation. Suppose θ is the phase signal to be measured, and the random phase error φ, which comes from the inherent randomness of quantum mechanics, follows a Gaussian distribution $D(\varphi) \propto \exp(-\frac{\varphi^2}{2\rho^2})$, where ρ is the standard deviation which is related to the polarization extinction ratio (PER) of the interferometer. The total sample number is N, so the phase uncertainty of the conventional measurement is (see details in Ref. [82])

$$\Delta\theta = \sqrt{\rho^2 + \frac{1}{N}}. \tag{8}$$

When we consider our WMPA scheme, the total phase uncertainty in this scenario is (see Eq. (A5) in Appendix A)

$$\Delta\theta_{\mathrm{w}} = \sqrt{16\delta^2\rho^2 + \frac{4}{N} + \left(\frac{\theta}{\delta}\right)^2 \Delta^2\delta}, \tag{9}$$

where $\Delta^2\delta$ is determined by the experimental device's precision. In our WMPA experiment, all the HWPs are mounted on stepper electric motors, whose accuracy $\Delta\alpha$ can reach as low as 0.44 mrad. $\Delta^2\delta$ has the same order of magnitude as $\Delta^2\alpha \sim 10^{-7}$ rad^2. And θ/δ has the same order of magnitude as $\kappa \sim 10^{-1}$ rad. With the help of weak measurement, the phase resolution of the interferometer can be improved by a factor of $1/(4\delta)$ (the same as the amplification factor) when $\rho \gg \sqrt{\frac{4}{N} + (\frac{\theta}{\delta})^2\Delta^2\delta}$. However, δ can not be infinitely small, in which case the third part of Eq. (A5) will play a major role, and the total phase uncertainty will get out of hand. The constraint on the magnification factor is dependent on the accuracy of the factor itself.

5. Conclusion

Although we only experimentally demonstrated the amplification of a polarization-dependent longitudinal phase, the general tasks of phase amplification can be readily realized by using Michelson interferometer suggested in Refs. [83,84]. This realization indicates that WMPA is capable of measuring any small phase signal with higher precision and sensitivity than the CM in practice.

In conclusion, we have described and demonstrated a weak measurements amplification protocol, i.e., WMPA that is capable of measuring any small longitudinal phase signal. The small phase introduced by LCVR is measured and one order of magnitude of amplification is realized. In our error analysis, the effect of magnification error is considered and we find that there is a trade-off between magnification and error. Larger amplification is possible if we consider cascading scenarios. The WMPA would have higher precision and sensitivity than the CM if the quantum noise limitation is negligible, which is usually the case in practice. In addition, the precision of our scheme has the potential to achieve the Heisenberg-limited precision scaling by using quantum resources such as squeezing states.[55] Our results significantly broaden the area of applications of weak measurements and may play a crucial role in high-precision measurements.

Appendix A: Phase uncertainty

Here we calculate the phase uncertainty of our scheme. Considering a realistic interferometer, the detection probability is

$$p = \frac{1}{2}(1 + \cos(\theta + \varphi)), \tag{A1}$$

where θ is the phase to be measured, and the random phase error φ satisfies Gaussian distribution: $D(\varphi) \propto \exp(-\frac{\varphi^2}{2\rho^2})$ with the standard derivation ρ. Given the total sample of N, the minimum uncertainty of the phase can be simplified as (see details in Ref. [82])

$$\Delta\theta = \sqrt{\rho^2 + \frac{1}{N}}. \tag{A2}$$

Our weak measurement scheme The detection probability is

$$p_{\mathrm{W}} = \frac{1}{2}(1 + \cos(\kappa + \varphi)), \tag{A3}$$

where κ can be calculated by Eq. (3) with $\alpha = \beta = 1/\sqrt{2}$ and $\gamma = \sin(45^\circ - 2\delta)$, $\eta = -\cos(45^\circ - 2\delta)$. Suppose $\theta \ll 1$ and δ is a small quantity, the amplified phase κ can be simplified with approximations as $\kappa = \theta/(4\delta)$. Because of the post-selection, the sample size has to multiply the success probability. So the total sample is changed from N to $N' = 4\delta^2 N$. The phase uncertainty can be calculated as

$$\begin{aligned}\Delta\theta_{\mathrm{w}} &= \left|\frac{\mathrm{d}\kappa}{\mathrm{d}p}\cdot\frac{\mathrm{d}\theta}{\mathrm{d}\kappa}\cdot\Delta p\right| = 4\delta\sqrt{\rho^2 + \frac{1}{N'}} \\ &= \sqrt{16\delta^2\rho^2 + \frac{4}{N}}.\end{aligned} \tag{A4}$$

However, Ref. [82] does not consider the uncertainty of magnification factors. As previously mentioned, the factor of amplification is mainly determined by the post-selection probability which is related to δ. The phase $\theta \simeq 4\delta\kappa$. According to the error transfer function, the phase uncertainty becomes

$$\begin{aligned}\Delta\theta_{\mathrm{w}} &= \sqrt{\left(\frac{\partial\theta}{\partial\kappa}\right)^2 \times \Delta^2\kappa + \left(\frac{\partial\theta}{\partial\delta}\right)^2 \times \Delta^2\delta} \\ &= \sqrt{16\delta^2\rho^2 + \frac{4}{N} + (4\kappa)^2\Delta^2\delta} \\ &= \sqrt{16\delta^2\rho^2 + \frac{4}{N} + \left(\frac{\theta}{\delta}\right)^2\Delta^2\delta}.\end{aligned} \tag{A5}$$

Appendix B: The calibration of the liquid crystal variable retarder

The LCVR causes a phase shift between the horizontal and vertical polarization states of photons when the voltage is introduced by a liquid crystal controller (Thorlabs LCC25). Here we give the calibration curve of the liquid crystal variable retarder (Thorlabs LCC1411-B) in Fig. B1. The phase shift of LCVR is linear with the voltage. However, the error bar of the phase shift θ increases gradually, which causes the error bar of the κ to become longer with the increase of the phase θ to be measured, see Fig. 3.

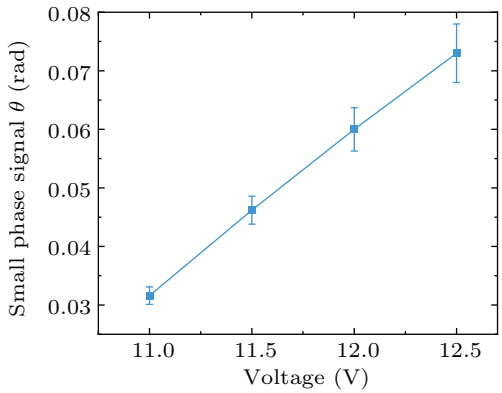


Fig. B1. The calibration curve of the LCVR.

Acknowledgements

Project supported by the National Natural Science Foundation of China (Grant Nos. 92065113, 11904357, 62075208, and 12174367), the Innovation Programme for Quantum Science and Technology (Grant No. 2021ZD0301604), and the National Key Research and Development Program of China (Grant No. 2021YFE0113100). This work was partially carried out at the USTC Center for Micro and Nanoscale Research and Fabrication. Meng-Jun Hu is supported by Beijing Academy of Quantum Information Sciences.

References

[1] Aharonov Y, Albert D Z and Vaidman L 1988 *Phys. Rev. Lett.* **60** 1351
[2] Dressel J, Malik M, Miatto F M, Jordan A N and Boyd R W 2014 *Rev. Mod. Phys.* **86** 307
[3] Jozsa R 2007 *Phys. Rev. A* **76** 044103
[4] Ritchie N W M, Story J G and Hulet R G 1991 *Phys. Rev. Lett.* **66** 1107
[5] Pryde G J, O'Brien J L, White A G, Ralph T C and Wiseman H M 2005 *Phys. Rev. Lett.* **94** 220405
[6] Kedem Y and Vaidman L 2010 *Phys. Rev. Lett.* **105** 230401
[7] Pusey M F 2014 *Phys. Rev. Lett.* **113** 200401
[8] Leggett A J 1989 *Phys. Rev. Lett.* **62** 2325
[9] Aharonov Y and Vaidman L 1989 *Phys. Rev. Lett.* **62** 2327
[10] Ferrie C and Combes J 2014 *Phys. Rev. Lett.* **113** 120404
[11] Brodutch A 2015 *Phys. Rev. Lett.* **114** 118901
[12] Cohen E 2017 *Found. Phys.* **47** 1261
[13] Kastner R 2017 *Found. Phys.* **47** 697
[14] Aharonov Y, Botero A, Popescu S, Reznik B and Tollaksen J 2009 *Phys. Lett. A* **301** 130
[15] Aharonov Y, Botero A, Popescu S, Reznik B and Tollaksen J 2009 *New J. Phys.* **11** 033011
[16] Pan A K 2020 *Phys. Rev. A* **102** 032206
[17] Lundeen J S, Sutherland B, Patel A, Stewart C and Bamber C 2011 *Nature* **474** 188
[18] Kim Y, Kim Y S, Lee S Y, Han S W, Moon S, Kim Y H and Cho Y W 2018 *Nat. Commun.* **9** 192
[19] Pan W W, Xu X Y, Kedem Y, Wang Q Q, Chen Z, Jan M, Sun K, Xu J S, Han Y J, Li C F and Guo G C 2019 *Phys. Rev. Lett.* **123** 150402
[20] Xu L, Xu H, Jiang T, Xu F, Zheng K, Wang B, Zhang A and Zhang L 2021 *Phys. Rev. Lett.* **127** 180401
[21] Hosten O and Kwiat P 2008 *Science* **319** 787
[22] Dixon P B, Starling D J, Jordan A N and Howell J C 2009 *Phys. Rev. Lett.* **102** 173601
[23] Tang T, Li J, Luo L, Shen J, Li C, Qin J, Bi L and Hou J 2019 *Opt. Express* **27** 17638
[24] Li S, Chen Z, Xie L, Liao Q, Zhou X, Chen Y and Lin X 2021 *Opt. Express* **29** 8777
[25] Huang J H, He F F, Duan X Y, Wang G J and Hu X Y 2022 *Phys. Rev. A* **105** 013718
[26] Goggin M, Almeida M, Barbieri M, Lanyon B, O'Brien J, White A and Pryde G 2011 *Proc. Natl. Acad. Sci. USA* **108** 1256
[27] Kocsis S, Braverman B, Ravets S, Stevens M, Mirin R, Shalm L and Steinberg A 2011 *Science* **332** 1170
[28] Yu S, Meng Y, Tang J S, Xu X Y, Wang Y T, Yin P, Ke Z J, Liu W, Li Z P, Yang Y Z, Chen G, Han Y J, Li C F and Guo G C 2020 *Phys. Rev. Lett.* **125** 240506
[29] Li Z P, Wang Y T, Yu S, Liu W, Meng Y, Yang Y Z, Wang Z A, Guo N J, Zeng X D, Tang J S, Li C F and Guo G C 2022 *Phys. Rev. A* **106** 012608
[30] Liu W T, Martínez-Rincón J and Howell J C 2019 *Phys. Rev. A* **100** 012125
[31] Monroe J T, Yunger Halpern N, Lee T and Murch K W 2021 *Phys. Rev. Lett.* **126** 100403
[32] Wu S and Li Y 2011 *Phys. Rev. A* **83** 052106
[33] Zhu X, Zhang Y, Pang S, Qiao C, Liu Q and Wu S 2011 *Phys. Rev. A* **84** 052111
[34] Nakamura K, Nishizawa A and Fujimoto M K 2012 *Phys. Rev. A* **85** 012113
[35] Kofman A, Ashhab S and Nori F 2012 *Phys. Rep.* **520** 43
[36] Aharonov Y and Vaidman L 1990 *Phys. Rev. A* **41** 11
[37] Pal M, Saha S, B S A, Dutta Gupta S and Ghosh N 2019 *Phys. Rev. A* **99** 032123
[38] Magaña Loaiza O S, Mirhosseini M, Rodenburg B and Boyd R W 2014 *Phys. Rev. Lett.* **112** 200401
[39] Zhou C, Zhong S, Ma K, Xu Y, Shi L and He Y 2020 *Phys. Rev. A* **102** 063717
[40] Bai X, Liu Y, Tang L, Zang Q, Li J, Lu W, Shi H, Sun X and Lu Y 2020 *Opt. Express* **28** 15284
[41] Luo L, He Y, Liu X, Li Z, Duan P and Zhang Z 2020 *Opt. Express* **28** 6408
[42] Wu Y, Liu S, Chen S, Luo H and Wen S 2022 *Opt. Lett.* **47** 846
[43] Feizpour A, Xing X and Steinberg A M 2011 *Phys. Rev. Lett.* **107** 133603
[44] Hallaji M, Feizpour A, Dmochowski G, Sinclair J and Steinberg A 2017 *Nat. Phys.* **13** 540
[45] Chen G, Aharon N, Sun Y N, Zhang Z, Zhang W H, He D Y, Tang J S, Xu X Y, Kedem Y, Li C F and Guo G C 2018 *Nat. Commun.* **9** 93
[46] Chen G, Aharon N, Sun Y N, Zhang Z, Zhang W H, He D Y, Tang J S, Xu X Y, Kedem Y, Li C F and Guo G C 2018 *Phys. Rev. Lett.* **121** 060506
[47] Starling D J, Dixon P B, Jordan A N and Howell J C 2010 *Phys. Rev. A* **82** 063822
[48] Steinmetz J, Lyons K, Song M, Cardenas J and Jordan A N 2022 *Opt. Express* **30** 3700
[49] Combes J, Ferrie C, Jiang Z and Caves C M 2014 *Phys. Rev. A* **89** 052117
[50] Ferrie C and Combes J 2014 *Phys. Rev. Lett.* **112** 040406
[51] Vaidman L 2014 arXiv:1402.0199 [quant-ph]
[52] Kedem Y 2014 arXiv:1402.1352 [quant-ph]
[53] Ferrie C and Combes J 2014 arXiv:1402.2954 [quant-ph]

[54] Knee G C and Gauger E M 2014 *Phys. Rev. X* **4** 011032
[55] Pang S and Brun T A 2015 *Phys. Rev. Lett.* **115** 120401
[56] Combes J, Ferrie C, Jiang Z and Caves C M 2014 *Phys. Rev. A* **89** 052117
[57] Tanaka S and Yamamoto N 2013 *Phys. Rev. A* **88** 042116
[58] Zhang L, Datta A and Walmsley I A 2015 *Phys. Rev. Lett.* **114** 210801
[59] Feizpour A, Xing X and Steinberg A M 2011 *Phys. Rev. Lett.* **107** 133603
[60] Sinclair J, Hallaji M, Steinberg A M, Tollaksen J and Jordan A N 2017 *Phys. Rev. A* **96** 052128
[61] Xia B, Huang J, Li H, Wang H and Zeng G 2023 *Nat. Commun.* **14** 1021
[62] Jordan A N, Martínez-Rincón J and Howell J C 2014 *Phys. Rev. X* **4** 011031
[63] Harris J, Boyd R W and Lundeen J S 2017 *Phys. Rev. Lett.* **118** 070802
[64] Xu L, Liu Z, Datta A, Knee G C, Lundeen J S, Lu Y Q and Zhang L 2020 *Phys. Rev. Lett.* **125** 080501
[65] Arvidsson-Shukur D, Halpern N Y, Lepage H V, Lasek A A, Barnes C and Lloyd S 2020 *Nat. Commun.* **11** 3775
[66] Chen G, Yin P, Zhang W H, Li G C, Li C F and Guo G C 2021 *Entropy* **23** 354
[67] Pang S, Dressel J and Brun T A 2014 *Phys. Rev. Lett.* **113** 030401
[68] Pang S and Brun T A 2015 *Phys. Rev. A* **92** 012120
[69] Dressel J, Lyons K, Jordan A N, Graham T M and Kwiat P G 2013 *Phys.Rev. A* **88** 023821
[70] Lyons K 2015 *Phys. Rev. Lett.* **114** 170801
[71] Wang Y T, Tang J S, Hu G, Wang J, Yu S, Zhou Z Q, Cheng Z D, Xu J S, Fang S Z, Wu Q L, Li C F and Guo G C 2016 *Phys. Rev. Lett.* **117** 230801
[72] Krafczyk C, Jordan A N, Goggin M E and Kwiat P G 2021 *Phys. Rev. Lett.* **126** 220801
[73] Kim Y, Yoo S Y and Kim Y H 2022 *Phys. Rev. Lett.* **128** 040503
[74] Martínez-Rincón J, Liu W T, Viza G I and Howell J C 2016 *Phys. Rev. Lett.* **116** 100803
[75] Martínez-Rincón J, Liu W T, Viza G I and Howell J C 2017 *Opt. Lett.* **42** 903
[76] Zhang C, Lai Y, Yang R, Liu K, Zhang J, Sun H and Gao J 2023 *Appl. Phys. Lett.* **122** 031107
[77] Huang J, Li Y, Fang C, Li H and Zeng G 2019 *Phys. Rev. A* **100** 012109
[78] Stárek R, Mičuda M, Hošák R, Ježek M and Fiurášek J 2020 *Opt. Express* **28** 34639
[79] Zhang Z H, Chen G, Xu X Y, Tang J S, Zhang W H, Han Y J, Li C F and Guo G C 2016 *Phys. Rev. A* **94** 053843
[80] Brunner N and Simon C 2010 *Phys. Rev. Lett.* **105** 010405
[81] Xu X Y, Kedem Y, Sun K, Vaidman L, Li C F and Guo G C 2013 *Phys. Rev. Lett.* **111** 033604
[82] Li L, Li Y, Zhang Y L, Yu S, Lu C Y, Liu N L, Zhang J and Pan J W 2018 *Phys. Rev. A* **97** 033851
[83] Hu M J and Zhang Y S 2017 arXiv:1707.00886 [quant-ph]
[84] Hu M J and Zhang Y S 2017 arXiv:1709.01218 [quant-ph]